Estimation of Effective Porosity and saturation volume by Extended Elastic Impedance approach: A case study

Sumit Verma, Samir Biswal, Reliance Industries Ltd., Mumbai, India

Introduction:

The study area is a gas field situated in the deepwater of east coast of India. The depositional setting is channel-levee complex. From seismic many smaller episodes of paleo-channel flow has been be distinguished within major channel-levee complexes. The smaller episodes of channels cut-fill and migrate, grow younger from bottom to top, depositing vertically offset sand bodies. Clean-thick channel sands, thinly laminated sands, splay sands and mudstone/shale are the major facies. In this complex geological setup both horizontal and vertical heterogeneity has been observed to a great extent. So the challenge in this field is to capture the reservoir heterogeneity efficiently. Any direct method of determining the reservoir property using transform based on single property viz., amplitude, sweetness, P-Impedance generate only an average outcome, which is devoid of finer details.

Effective porosity and saturation are the key reservoir parameter which plays a vital role in reserve estimation and planning production operations. In the present study extended elastic impedance approach has been adopted for obtaining effective porosity and saturation (Arsalan et al, 2009). Results show that EEI approach is an effective way of deriving petrophysical properties. The output of this study can be effectively used for static model building and volumetric calculation; hence helpful in further field development.

Theory:

Two-term linearization of Zeoppritz equation for reflectivity (Aki & Richards 1980),

$$R=A+B\sin^2\theta \qquad (1)$$

replacing $\sin^2\theta$ by $\tan\chi$ in the two-term AVO equation, allows angle to vary form -90° to +90°,

$$R(\chi) = A + B\tan\chi \qquad (2)$$

Whitecombe et al. extended the concept of elastic impedance (Connolly, 1999), that can be used for fluid and lithology mapping. EEI is defined as

$$EEI(\chi) = \alpha_0^{p}\rho_0^{q}\left[\left(\frac{\alpha}{\alpha_0}\right)^{p}\left(\frac{\beta}{\beta_0}\right)^{q}\left(\frac{\rho}{\rho_0}\right)^{r}\right] \qquad (3)$$

where α = P-wave velocity, β = S-wave velocity, ρ = density, $p = \cos\chi + \sin\chi$, $q = -8K\sin\chi$, and $r = (\cos\chi - 4K\sin\chi)$, α_0, β_0, and ρ_0 are the average of the respective property used as normalization factors for P velocity, S velocity, and density, respectively. K is the average of $(V_S/V_P)^2$ in the time/depth interval.

Methodology:

In the present study, petrophysical properties (effective porosity and saturation) estimation was done in the sequence employed by Arsalan et al, 2009. In the first step EEI was computed at different angles χ using equation (3), taking P Sonic, S Sonic and Density logs as input. Further, angle χ_{ϕ} (and χ_{Sw}) against maximum absolute correlation of computed EEI log and Effective Porosity (ϕ_{eff}) (and saturation (Sw)) log was determined. The next step was to compute AVO intercept (A) and gradient (B) from seismic gather. Further, equivalent seismic volumes were calculated using equation (2) at angles χ_{ϕ} and χ_{Sw}, which have been obtained in the first step. These equivalent seismic volumes were inverted using constrained sparse spike inversion algorithm. The inversion products are EEI volume corresponding to porosity and saturation at χ_{ϕ} and χ_{Sw} angles respectively. These were then scaled to derive porosity and saturation volumes.

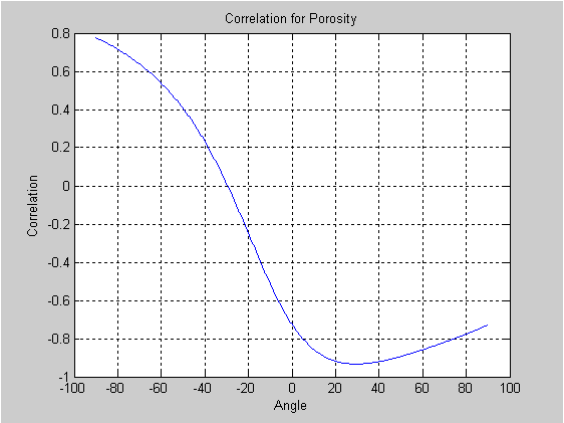

Figure 1a: Correlation for Effective Porosity (ϕ_{eff}).

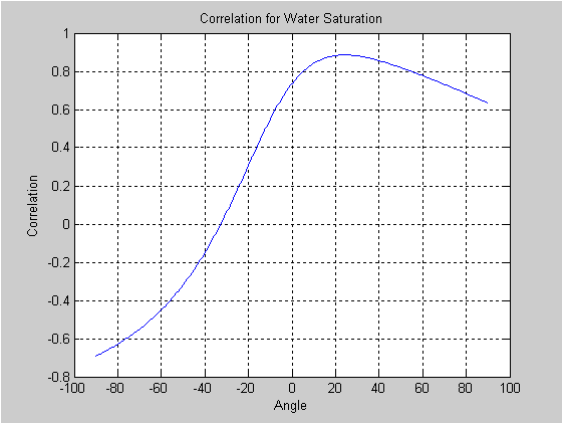

Figure 1b: Correlation for Saturation (Sw)

For Effective Porosity	
Angle χ_{ϕ} = **27.5 °**	Correlation = **93%**

Table: 1 (a)

For Saturation	
Angle χ_{Sw} = **24 °**	Correlation = **89%**

Table : 1 (b)

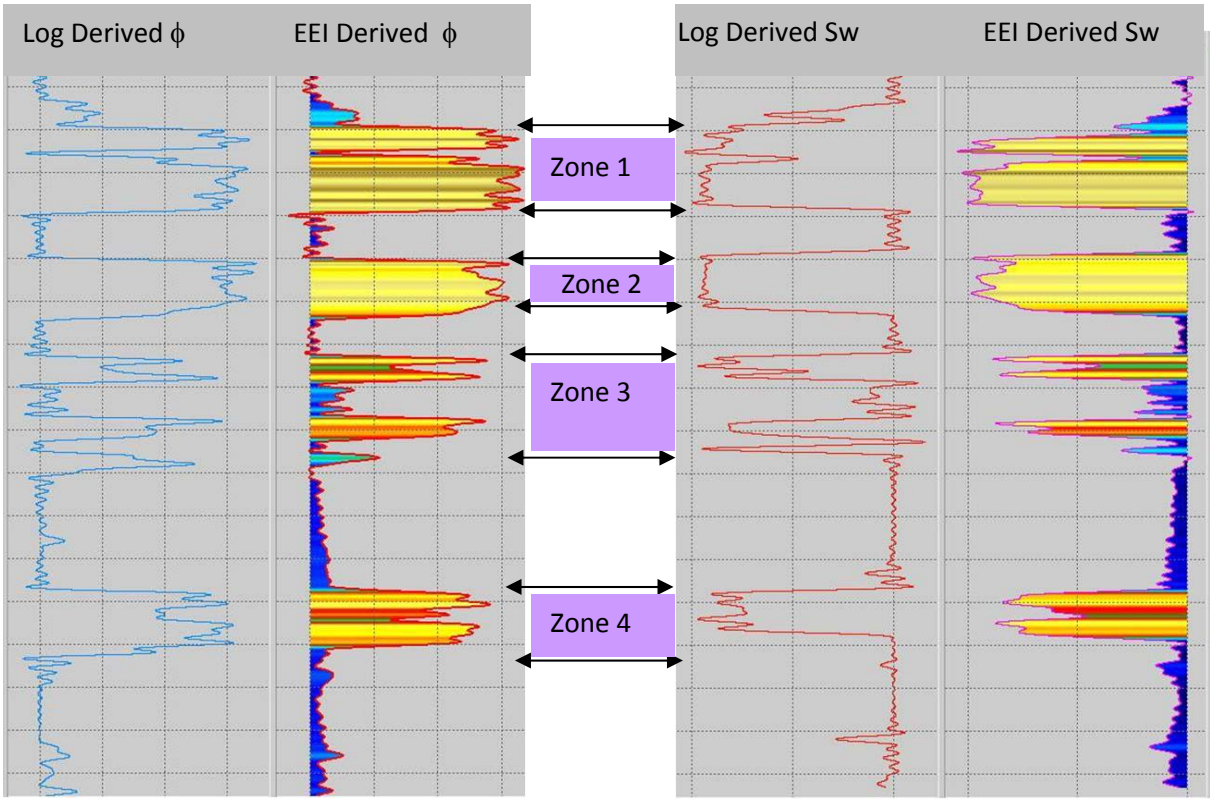

Figure 2a Comparison of log derived and EEI derived Effective Porosity

Figure 2b Comparison of log derived and EEI derived Saturation

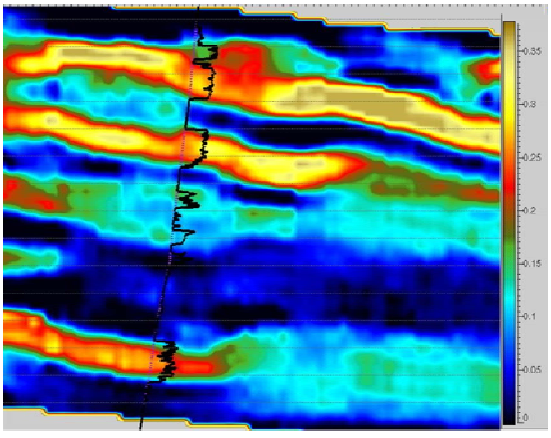

Figure3a: Section showing Effective Porosity

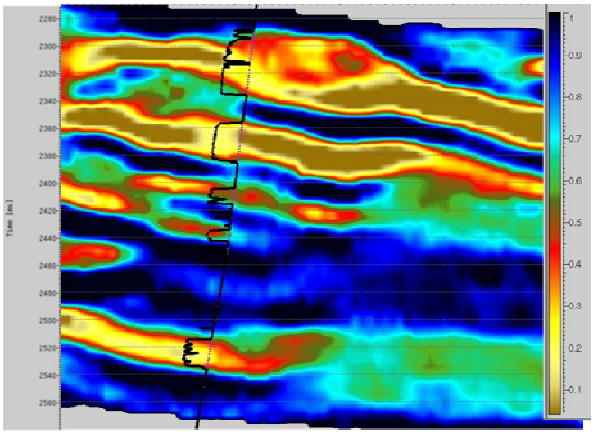

Figure3b: Section showing saturation (S_g)

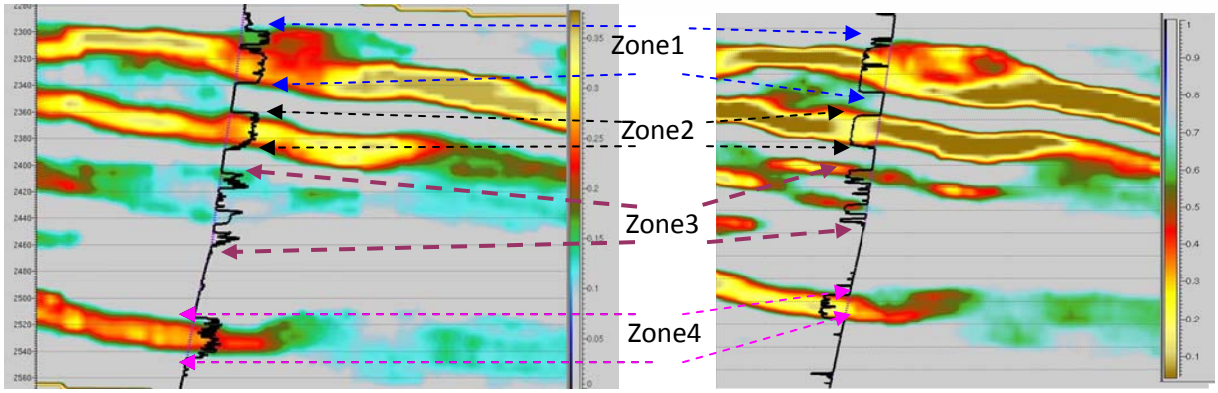

Figure 4a: Section showing ϕ_{eff} with 10% cut off

Figure 4b: Section showing Sw volume with 70% cut off

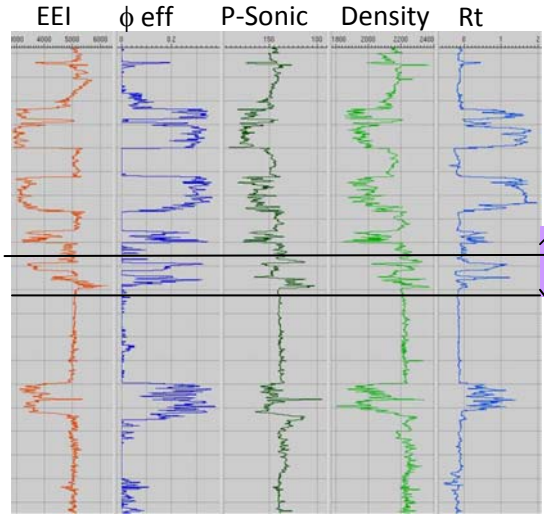

Figure 5a. Log

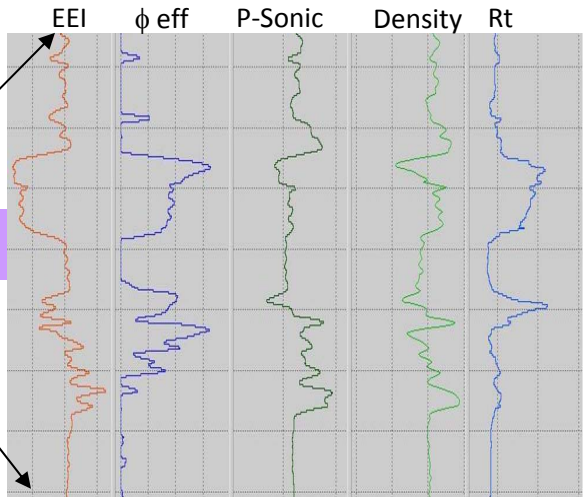

Figure5b. Zoomed portion of lower part of zone 3

Result:

Correlations between Effective Porosity log and saturation log with EEI log for various angles are obtained and plotted in figure 1a and 1b. EEI corresponding to $\chi = 27.5°$ gives the maximum correlation (≈93%) with log-derived Effective Porosity. The optimum χ and the corresponding correlation values for Effective Porosity and saturation log are given in Table 1(a) and Table 1(b).

Figure 2a & 2b, compares pseudo-petrophysical property logs (ϕ_{eff} & S_W) derived from EEI and corresponding actual petrophysical logs (ϕ_{eff} & S_W). A very good match, except for a scaling factor, indicates that the petrophysical volumes derived from seismic data through EEI can be used for quantitative interpretation.

Figure 3a & 3b, shows the section view of generated EEI petrophysical properties, ϕ_{eff} & S_W respectively through the well. Actual well log overlaid on the section indicates their match at the well and the property distribution away from the well. Thus, the EEI-derived volumes help in mapping the character of reservoir sand in 3D space and further quantitative reservoir characterization.

Discussions:

Close observation of EEI, Effective porosity, P-sonic, density and resistivity logs, Fig-3a, 3b, 4a, 4b, 5a & 5b, it is found that, the first, second and the forth zone of sand are clearly indicated by low EEI value on the log, and in the third zone the upper sand is giving low EEI value but the lower portion of this although having a good effective porosity, is unable to be captured in EEI log. The most likely reason is that the zone 1, 2 and 3 are channel sand with minimal laminations of shale, whereas the lower portion of third zone is mostly laminated sand of levy area. The thickness of the laminated sands is beyond seismic resolution for the bandwidth of the available seismic data.

References:

Arsalan, S., and Yadav, A., 2009, Application of extended elastic impedance: A case study from Krishna-Godavari Basin, India, The Leading Edge, October issue,1204-1209.

Whitecombe, D., Conolly, P., Reagan, R. and Redshaw,T., Extended elastic impedance for fluid and lithology prediction,Geophysics,**67**, 63-67.

Conolly, P.,1999, Elastic Impedance, The Leading Edge, April issue, 438-452.